Molecular Crystals and Liquid Crystals
Publication details, including instructions for authors and subscription information:
http://www.tandfonline.com/loi/gmcl18

Thermodynamic Characterization of the Influence of Ca^{2+} on Dilauroylphosphatidylethanolamine, Dipamitoylphosphatidylglycerol, and Dipamitoylphosphatidylcholine

J. Phiri [a], D. Patterson [a], J. M. Collins [a], P. J. Quinn [b], W. Tamura-lis [c] & L. J. Lis [d]

[a] Department of Physics, Marquette University, Milwaukee, WI, 53233

[b] Department of Biochemistry, King's College London, London, W87AH, U.K.

[c] Dept. of Obstetrics and Gynecology, Univ. of Nebraska Medical Center, Omaha, NE, 68105-1065

[d] Division of Oncology/Hematology, The Chicago Medical School and the VA Medical Center, North Chicago, IL, 60064

Version of record first published: 24 Sep 2006.

To cite this article: J. Phiri , D. Patterson , J. M. Collins , P. J. Quinn , W. Tamura-lis & L. J. Lis (1991): Thermodynamic Characterization of the Influence of Ca^{2+} on Dilauroylphosphatidylethanolamine, Dipamitoylphosphatidylglycerol, and Dipamitoylphosphatidylcholine, Molecular Crystals and Liquid Crystals, 195:1, 77-91

To link to this article: http://dx.doi.org/10.1080/00268949108030892

Mol. Cryst. Liq. Cryst., 1991, Vol. 195, pp. 77–91
Reprints available directly from the publisher
Photocopying permitted by license only

Printed in the United States of America

Thermodynamic Characterization of the Influence of Ca^{2+} on Dilauroylphosphatidylethanolamine, Dipalmitoylphosphatidylglycerol, and Dipalmitoylphosphatidylcholine

J. PHIRI, D. PATTERSON and J. M. COLLINS

Department of Physics, Marquette University, Milwaukee, WI 53233

and

P. J. QUINN

Department of Biochemistry, King's College London, London W87AH U.K.

and

W. TAMURA-LIS

Dept. of Obstetrics and Gynecology, Univ. of Nebraska Medical Center, Omaha, NE 68105-1065

and

L. J. LIS

Division of Oncology/Hematology, The Chicago Medical School and the VA Medical Center, North Chicago, IL 60064

(*Received April 1, 1990; in final form July 12, 1990*)

The thermodynamic properties of dipalmitoylphosphatidylcholine (DPPC), dipalmitoylphosphatidylglycerol (DPPG) and dilauroylphosphatidylethanolamine (DLPE) dispersed in water and low molarity $CaCl_2$ solutions are described. In all cases, the subgel phase was induced to aid further thermodynamic comparisons. The interaction of Ca^{2+} with DPPC is responsible for a reduction in the transition enthalpy of the subgel-to-gel bilayer transition with increasing $CaCl_2$ concentration, while the presence of a very small concentration of $CaCl_2$ eliminates the sub and pre-transitions for DPPG bilayers and shifts the main transition temperature upward by 40°C. The Ca^{2+} interaction with DLPE appears to be biphasic. Low molarity $CaCl_2$ solutions cause the main transition to become less thermodynamically distinct with low transition enthalpies. However, in the presence of 50 mM $CaCl_2$, DLPE bilayers underwent two

phase transitions, as was observed for DLPE, in water but at different temperatures. Static and real time x-ray diffraction experiments are used, in part, in the interpretation of these calorimetry observations.

Keywords: Ca^{2+} interactions with phospholipids, dilauroylphosphatidylethanolamine, dipalmitoylphosphatidylglycerol, calorimetry, x-ray diffraction, synchrotron radiation

INTRODUCTION

The structure and function of biological membranes and lipid systems are clearly dependent on the solvent character in contact with the lipid headgroups.[1-5] Divalent ions have been shown to influence the structure and packing of a variety of neutral[6-11] and charged[12-17] phospholipid model membranes. Negatively charged phospholipids are of particular interest from the point of view of a possible functional role for phospholipids in membranes, since both their phase transition characteristics and bilayer structures are responsive to changes in the ionic environment.[12-17] This provides a potential membrane trigger mechanism initiated by changes in the surface pH, or concentration of monovalent or divalent ions. Divalent ions such as Ca^{2+} have been shown[6-9] to bind to phosphatidylcholines, thereby imparting a surface charge to the phospholipid headgroup region. This interaction may also have physiological importance. Few studies, however, have focused on the interaction of these ions with saturated chain phosphatidylethanolamines.[18-20] This is particularly surprising since Ca^{2+} has been shown to bind to phosphatidylcholines at solution concentrations as low as 1 mM.[6-9] It has additionally been shown that the dilauroyl derivative of phosphatidylethanolamine in water has a variety of metastable and hysteretic phases which depend on the thermal equilibration of the sample.[21,22] It is relevant therefore to ascertain not only whether Ca^{2+} binds to phosphatidylethanolamine, either modifying the charge at the lipid-water interface or the packing structure of the lipids within the bilayer, but also to determine the role, if any, that divalent ions have on the stability and thermal hysteresis of phosphatidylethanolamine phase structure.

Phosphatidylglycerol is a negatively charged phospholipid found at high concentrations in the plasma membrane of microorganisms, in the chloroplast membranes in plants, and in lung surfactant. The influence of divalent cations, particularly Ca^{2+}, has been examined for a number of synthetic phosphatidylglycerols.[15-17,23-25] The structures and phase transitions have been reported in detail, primarily with regard to the gel and liquid crystalline bilayer states. Complexation, acyl chain tilt, and phase metastability have been described. However, it has recently been shown that a subgel phase can be induced for DPPG in water[26,27] in a manner similar to that observed for DPPC in water. This finding provides a clear starting point for characterization studies and an explanation for previously observed metastable behavior.

We have previously reported on the influence of Ca^{2+} on the DLPE and DMPE gel phase structure using x-ray diffraction and Raman spectroscopy.[20] There was no apparent effect on the gel phase bilayer structure or packing when low $CaCl_2$ concentrations were used. The influence of Ca^{2+} on the phases present in the ester

fused lipid dihexadecylphosphatidylethanolamine (DHPE) has also been reported. At high pH and in the presence of $CaCl_2$, DHPE has been shown to form a single phase system consisting of the H_{II} packing of cylinders.[18,19] In this report we examine the interaction of low molar solutions of $CaCl_2$ on the DLPE and DPPG phase transitions using calorimetry. The lipids were chosen because of their complex phase behavior in water and their ability to form subgel phases. It is important to use a beginning phase which is an equilibrium phase to insure reproducibility between experimental groups. The subgel phase may also have biological significance under cryogenic conditions. Some of these systems were also examined using static and real time x-ray diffraction techniques. Comparisons are also made with our previous studies of the influence of Ca^{2+} on DPPC phase transition phenomena[6-11,28] and real time x-ray diffraction studies of the phase transitions of these lipids in water.[29]

MATERIALS AND METHODS

Phospholipids were obtained from Avanti Polar Lipids (Birmingham, AL) and used without further purification. Zero to 50 mM $CaCl_2$ solutions in water were added to the dry lipid mixture to give 80 wt% (water/lipid + water) for both x-ray diffraction and calorimetric examination. The samples were heated above their transition temperature for one hour and then stored at 0°C for at least one week. The resulting samples visually appeared to be homogeneous lipid-water mixtures with no evidence of residual lipid powder. This equilibration technique provided more time than usually required for the formation of the subgel phase. It has been previously shown[8] that structural parameters for similarly prepared samples were not influenced by the presence of inferred ion gradients within the lipid multilamellar arrays. Samples for calorimetric examination were hermetically sealed in aluminum pans.

Transition temperatures and enthalpies were measured by a Perkin-Elmer DSC-2C. Analyses of the measured thermograms were made with a Perkin-Elmer Thermal Analysis Data Station (TADS). Enthalpy per unit area was calibrated using indium (99.999% pure). At least two samples were examined for each $CaCl_2$ concentration and lipid used. Samples were also subjected to the above equilibration procedure after initial DSC examination in order to insure reproducibility of the results observed during the initial DSC scan. Experimental uncertainties in the enthalpy determination were obtained from differences in results obtained for different samples as well as the reproducibility of these values for independent determinations for each endotherm. The latter calculations vary, to some extent, due to differences where one chooses the beginning and end of each endotherm. Our estimate of a *ca* 5% uncertainty is a measure of these factors. However, the trends observed in this study were not affected by the use of this uncertainty. It should also be noted that the measured transition enthalpies include heats of transfer for the flow of water and ions into the interbilayer region between bilayers as transitions proceed. In each case the disordering of the lipid acyl chains increases the area per headgroup at the bilayer interface resulting in a greater hydration

requirement. This phenomenon occurs in all lipid solvent systems including pure water. Transition temperatures were reproducible to ±1°. The heating and cooling rates were 2.5°C/min for all samples and calibrations. We found no effect of scan rate on the relative effects of ions on the thermodynamic parameters.

The static x-ray samples were exposed to nickel filtered CuK_α ($\lambda = 0.154$ nm) radiation. The x-ray patterns were collected photographically using modified Guinier Type Cameras. Bragg diffraction was used to measure the bilayer repeat distance (d-spacing) and acyl chain packing parameters. Powdered Teflon was used as an internal standard in these measurements. The temperature of the sample was controlled by a circulating water bath. Typical exposure times were over 24 hours.

X-ray diffraction patterns were also obtained using the 0.15 nm x-radiation at station 7.2/3 of the synchrotron radiation source of the SERC Daresbury (UK) Laboratory.[3-10] A cylindrically bent single crystal of Ge^{31} and a long float mirror were used for monochromatization and horizontal focussing, providing about 2×10^9 photons $- s^{-1}$ down a 0.2 mm collinator at 2.0 GeV and 100 to 200 mA of electron beam current. A Keele University flat plate camera was used with a sample path of 1 mm. Scattered x-rays were recorded on a linear detector constructed at the Daresbury Laboratory. The lead time between data acquisition frames was 50 μs with a temporal resolution of 2 s for each frame. X-ray scattering has been plotted as a function of reciprocal space ($S = 1/d = 2 \sin\theta/2$) using Teflon ($d = 0.48$ nm) as a calibration standard.[32] All mesophase and subcell spacings were calculated using Bragg's Law. Temperature scans were produced by water baths connected internally to the sample mount of the x-ray camera. The temperature of the sample was monitored internally using a thermocouple placed adjacent to the sample in the x-ray sample holder.

RESULTS AND DISCUSSION

DPPC

The interaction between Ca^{2+} and phosphatidylcholines has been extensively characterized. Ca^{2+} binds to the phosphatidylcholine headgroup thereby destroying the zwitterionic character of the lipid and producing a charged bilayer surface.[6-9] It has been previously shown that fully hydrated DPPC undergoes the $L_c \langle = \rangle L_\beta \langle = \rangle P_\beta \langle = \rangle L_\alpha$ phase sequence during a continuous temperature scan.[29] Bilayer phases with tilted acyl chains ($L_{\beta'}$ and $P_{\beta'}$) require further temporal equilibration in order to be induced. It has recently been shown[28] that this phase sequence was modified in the presence of $CaCl_2$. The "pre-transition" calorimetry peak transition involved a continuous expansion of the L_β packing structure rather than the transition from the gel state (L_β) bilayer to the rippled phase (P_β or $P_{\beta'}$). In addition, the measured enthalpy for the $L_c \rightarrow L_\beta$ transition in DPPC decreased until it was not measurable as the $CaCl_2$ concentration increased from 0 to 50 mM $CaCl_2$. There was, however, essentially no change in the sub, pre, or main transition temperatures and the pre- and main transition enthalpies. These results are summarized in Table I.

TABLE I

Thermodynamic parameters for the initial heating scans of multi-lamellar arrays of dipalmitoylphosphatidylcholine in various $CaCl_2$ solutions. Transition temperatures and enthalpies are subscripted 1, 2, or 3 to indicate the first, second, or third endothermic peak observed on heating as determined from the calorimeter tracing of the initial heating scans. Typically (see text for more details), the first transition is the sub or $L_c \rightarrow L_\beta$ transition, the second is the pre- or $L_\beta \rightarrow P_B$ transition, and the third is the main or $P_B \rightarrow L_\alpha$ transition. All samples were initially equilibrated as described in the *Materials and Methods*.

$[CaCl_2]$ mM	T_1 (K)	ΔH_1 (kcal/mole)	T_2 (K)	ΔH_2 (kcal/mole)	T_3 (K)	ΔH_3 (kcal/mole)
0	294.0	2.5	308.3	1.0	314.3	7.3
10	291.7	3.6	303.1	1.4	312.8	9.7
20	293.6	3.3	308.9	0.9	314.3	7.8
30	289.8	2.4	307.0	1.0	313.1	7.9
40	293.6	1.1	308.2	0.9	314.8	7.6
50	--	--	309.8	1.1	314.8	8.3

DLPE

The phase characterization of fully hydrated DLPE in water after a variety of equilibration schemes has been previously described.[21,22] Equilibration of the system at or above room temperature has been shown to induce four different lamellar phases designated β_1, β_2, L_β and L_α. The L_β and L_α phases are the typical gel and liquid crystalline bilayer phases with the L_β form induced upon cooling from the L_α phase. The β_1 and β_2 phases are crystalline bilayers induced by equilibration for extended periods at 26° and 32°C, respectively. However, if the sample is equilibrated at 0°C for over one week, then a different crystalline bilayer phase designated as L_c is formed (Figure 1 and Table II). The L_c phase produces different acyl chain x-ray diffraction peaks than the β_1 and β_2 phases indicating that each phase (β_1, β_2 and L_c) contains different acyl chain packing subcells.

Table III shows thermodynamic data obtained for DLPE in H_2O after the samples were equilibrated at 0°C for over one week. DLPE in H_2O underwent two endothermic transitions between the subgel or L_c phase and the L_α phase as determined by calorimetry. Static and real time x-ray diffraction measurements of the phase transitions experienced by DLPE in water were used to examine the above transitions. In contrast to our calorimetric examination of this system which showed two thermal transitions (Table I), only one structural transition was observed using real time x-ray diffraction (Figure 1) corresponding to that observed calorimetrically at 306 K between the L_c and L_α phases. No structural changes (mesophase or acyl

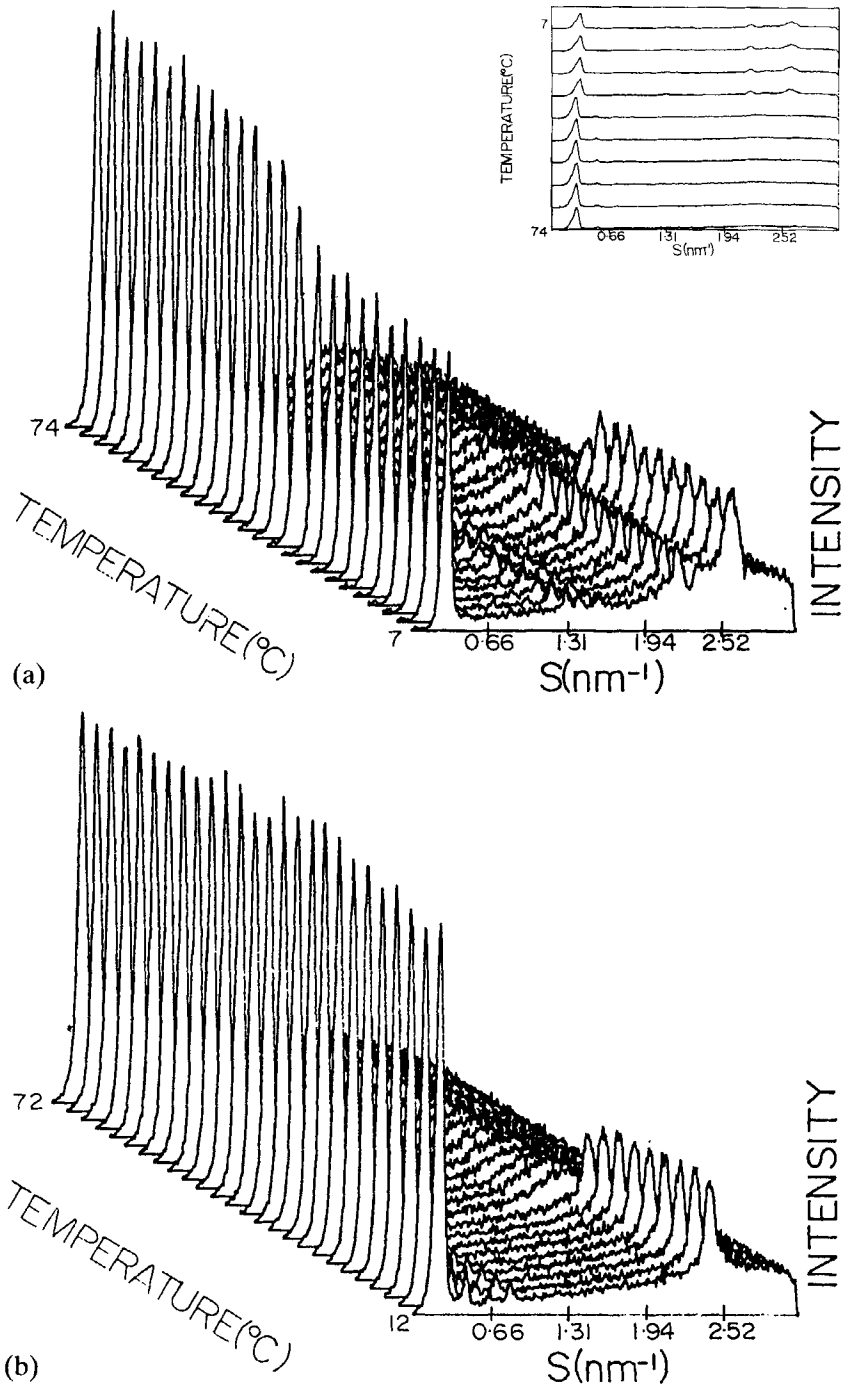

FIGURE 1 X-ray diffraction patterns collected for DLPE in water undergoing (a) an initial linear heating scan of ~7.4°C/min and (b) a linear re-heating scan of ~7.2°C/min. Every tenth frame of 2s duration of a total data set of 255 frames is shown. *Insets.* Every twenty-fifth frame of the data set is plotted as a function of reciprocal space.

TABLE II

Thermodynamic parameters for the initial heating scans for multi-lamellar arrays of dilauroylphosphatidylethanolamine in various $CaCl_2$ solutions. Transition temperatures and enthalpies are subcripted 1 or 2 to indicate the first or second endothermic peak observed on heating as determined from the calorimeter tracing of the initial heating scans (see text for structural interpretations). All samples were equilibrated at ~0°C for over one week before examination.

mM $CaCl_2$	T_1 (K)	ΔH_1 (kcal/mole)	T_2 (K)	ΔH_2 (kcal/mole)
0	306.0	11.3	315.4	2.4
10	310.5	2.6		
20	310.9	1.0		
30	314.8	1.4		
40	313.6	3.0		
50	303.7	0.6	306.8	6.9

chain) were observed in this system at a temperature of 315 K or higher. The L_c phase was observed to evolve into the L_α phase upon initial heating in a two-state or first-order process. The subsequent transition at ~302 K between the L_β and L_α phases observed during a reheating cycle proceeded similarly via a two state process. The DLPE in water $L_c \rightarrow L_\alpha$ phase transition was observed in static, equilibrium experiments (Table IV) to occur in the temperature region near ~315°K with no structural transitions observed near ~306°K. These results are directly opposite to those obtained by our real time (non-equilibrium) x-ray diffraction study. The combination of the above static and real time x-ray diffraction experiments can be used to interpret the presence of the two calorimetrically observed

TABLE III

Structural parameters determined from real time x-ray diffraction patterns for the various phase states formed by DLPE in H_2O.

Phase	Mesophase Spacing (nm)	Acyl Chain Peaks (nm)
L_c	3.10	0.381 0.418 0.452 0.472
L_α	3.94	0.445
L_β	4.62	0.410 to 0.419

TABLE IV

X-ray structural parameters for dilauroylphosphatidylethanolamine in various $CaCl_2$ concentrations as a function of temperature during initial heating and cooling. All data came from static x-ray patterns.

$[CaCl_2]$ (mM)	Temperature °C	Mesophase d spacing (nm)	Acyl chain repeat spacing (nm)
0	18.5	4.54	0.459 0.434 0.418 0.395
	31.0	4.54	0.464 0.453 0.422 0.413 0.395
	37.2	4.46	0.468 0.459 0.436 0.416 0.395
	51.9	4.27	—
	37.7	4.60	0.469 0.458 0.435 0.417 0.396
	31.4	4.57	0.464 0.454 0.430 0.414 0.392
	19.9	4.51	0.469 0.460 0.435 0.420 0.397
10	26.0	4.61	0.456 0.436 0.415 0.393
	47.2	4.17	—
	26.2	4.57	0.444 0.399 0.378

TABLE IV (continued)

$[CaCl_2]$ (mM)	Temperature °C	Mesophase d spacing (nm)	Acyl chain repeat spacing (nm)
20	26.0	4.51	0.437 0.414 0.398 0.377
	47.2	4.30	—
	27.0	4.52	—
30	33.0	4.51	0.453 0.423 0.402
	51.0	4.39	—
	31.2	4.30	0.416 0.399
40	33.0	4.57	0.436 0.413 0.398 0.377
	51.0	4.47	—
	31.2	4.52	0.443 0.421 0.405 0.384
50	18.5	4.47	0.436 0.413 0.399 0.377
	31.0	4.44	0.437 0.397 0.377
	37.2	4.46	0.434 0.396 0.376
	51.2	4.20	—
	37.7	4.51	0.462 0.438 0.376
	31.4	4.54	0.399 0.377
	19.9	4.45	0.398 0.377

phase transitions between the L_c and L_α phases in the system. It can be inferred that each calorimetric peak is representative of an $L_c \rightarrow L_\alpha$ phase transition with the lower temperature transition (at ~306°K) due to a sample population which can kinetically transform at a faster rate than a sample population, as indicated by the ~315°K transition, which transforms more slowly. The cause of these different sample populations in our calorimetry samples is not clear, although one cannot rule out that the lipid directly in contact with the aluminum pan may have different kinetic requirements for the $L_c \rightarrow L_\alpha$ transition than portions of the sample that are not in contact with the aluminum pan.

Samples of DLPE in 10–50 mM $CaCl_2$ solutions were also examined calorimetrically (Table III). The presence of 10–40 mM $CaCl_2$, caused DLPE bilayers to undergo a single, typically broad, transition. The DLPE transition temperature and enthalpy was essentially constant with $CaCl_2$ concentrations varying from 10–40 mM. The observed enthalpies were, however, lower than the combined enthalpies for the transitions observed for DLPE in water with that observed for 20 mM $CaCl_2$ being the lowest observed enthalpy. When 50 mM $CaCl_2$ was present, the DLPE main phase transition temperature was ~307°K, the peak became better defined and the enthalpy increased to 6.9 Kcal/mole. However, a much smaller peak was also observed at ~304°K with a transition enthalpy of 0.6 Kcal/mole. These results clearly show that Ca^{2+} interacts with DLPE. This interaction is more pronounced thermodynamically than that for phosphatidylcholine in $CaCl_2$. It is also clear that DLPE in the subgel phase must be used as the equilibrium starting point since similar studies had not previously shown any interaction between DLPE and Ca^{2+} in the L_β or L_α phases.

Static x-ray diffraction patterns were also obtained for samples of DLPE in 0–50 mM $CaCl_2$ solutions as a function of temperature. It was impossible to exactly mimic the above calorimetry scans since equilibrating DLPE samples at various temperatures has been previously shown[21] to form a number of unique metastable phases. As discussed previously, the β_1 and β_2 crystalline bilayer phases have been formed by DLPE in water when equilibrated for extended periods at 26° and 32°C respectively, while the L_c crystalline bilayer phase has been formed by equilibrating DLPE in water for extended periods at 0°C. Mesophase bilayer repeat spacings and acyl chain diffraction peaks for DLPE in water and various $CaCl_2$ solutions as a function of temperature are shown in Table IV. The DLPE L_c phase was observed at the lowest temperature studied when water was present. The DLPE β_1 phase was produced when this sample was heated to between 30 and 40°C and subsequently cooled below 40°C during the course of our data collection. The highest temperature used to examine this sample was 52°C. However, the acyl chain peaks at this temperature were weak, which is consistent with the formation of disordered acyl chains or the L_α phase.

Samples of DLPE in various $CaCl_2$ concentrations were examined at an initial temperature below the calorimetrically determined acyl chain melting phase transition temperature (T_m), a temperature above T_m, and subsequent cooling to another temperature below T_m as determined from data in Table II. Crystalline bilayer phases were formed as a starting point in each sample which were similar in their acyl chain diffraction peaks to that produced by the L_c phase of DLPE in water.

The DLPE high temperature structures can be inferred, as discussed previously, to be in the L_α phase when 10–50 mM $CaCl_2$ was present, while a crystalline bilayer phase appeared to form on subsequent cooling to a temperature below T_m when 10, 30, and 40 mM $CaCl_2$ were present. The acyl chain packing of the subsequently cooled bilayer structure produced in DLPE when 20 mM $CaCl_2$ was present could not be deduced since the wide angle scattering was weak. This finding is consistent with the calorimetric data for DLPE in 20 mM $CaCl_2$ shown in Table II which indicate an $L_c \rightarrow L_\alpha$ phase transition which has a very low enthalpy. It can be hypothesized that the L_α phase packing may be present on supercooling since there is a small $L_c \rightarrow L_\alpha$ transition enthalpy which is indicative of little difference in the thermal energies of the L_c and L_α phases. The static x-ray diffraction data (Table III) for DLPE in 50 mM $CaCl_2$ was consistent with the calorimetric determination (Table II) of two (rather than the one produced when 10–40 mM $CaCl_2$ was present) phase transitions at ~30 and 33°C.

DPPG

DPPG bilayers dispersed in water have been examined by calorimetry and x-ray diffraction. The initial heating calorimetry scan for DPPG in water shows the presence of three endotherms which can be correlated to four phases undergoing sub-, pre- and main phase transitions, as deduced from similar scans for DPPG in water (Figure 2, Table V). Upon subsequent cooling and re-heating, only the pre- and main phase transitions are reversible. These phase transitions have been examined in detail using real time x-ray diffraction (Figure 3 and Table VI). To clarify the above calorimetry results, an initial DPPG in water subgel phase was verified by a static x-ray pattern taken at 0°C. Real time x-ray diffraction done on this system with this initial subgel phase clearly indicated the acyl chain transitions involved in the sub and main phase transitions. The subgel to gel phase transition (Figure 3) involved a second order continuous transition in the acyl chain packing from a rectangular subcell into a hexagonal subcell (Table VI). The gel to liquid crystalline phase transition proceeded by a first order or two state transition mechanism (Figure 3) between subcells characterized in Table VI. The pre-transition was observed (Figure 3) to involve a continuous expansion of the acyl chain packing from 0.406 to 0.415 nm. Upon cooling, the subgel phase was again induced in this system. Similar acyl chain transitions were observed for sub-, pre- and main phase transitions on reheating, as observed in the initial heating (Figure 3). These observations (Figure 3) indicated the presence of a sub-transition of low enthalpy on reheating which was not apparent in the calorimetry scan (Figure 2). The phase transitions for this system can be thus deduced as involving the phase sequence: $L_c \langle = \rangle L_{\beta_1} \langle = \rangle L_{\beta_2} \langle = \rangle L_\alpha$, where the transition from the gel to subgel phase requires long periods of time.

The phase transitions for DPPG in 0–50 mM $CaCl_2$ were examined in the temperature range 275–360°K (Table V and Figure 2). DPPG in 10 mM $CaCl_2$ produced a single endotherm at approximately 355°K which is 40° greater than that of the main transition observed for DPPG in water. The presence of higher $CaCl_2$ con-

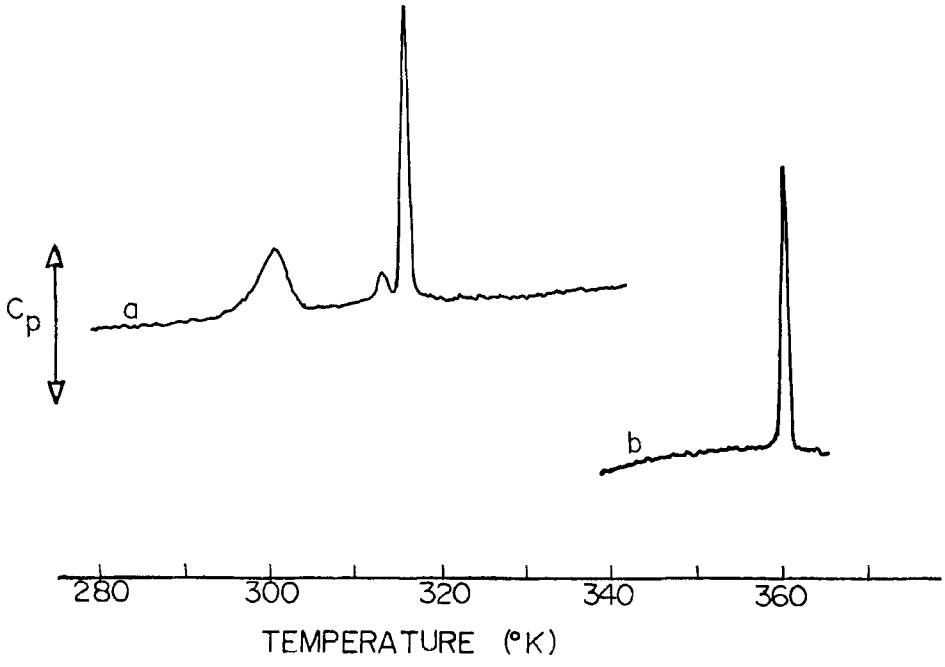

FIGURE 2 Differential scanning calorimetry scans for the initial heating of dipalmitoylphosphatidylglycerol in (a) 0 and (b) 10 mM $CaCl_2$. Samples were equilibrated at ~273°K (0°C) for approximately one week before examination. The temperature scan rate was 2.5 K/min. The scale for the specific heat at constant pressure (C_p) is in cal/gm/K. Upward changes in the calorimeter tracings are due to positive changes in C_p.

TABLE V

Thermodynamic parameters for multi-lamellar arrays of dipalmitoylphosphatidylglycerol in 0-10mM $CaCl_2$. Transition temperatures and enthalpies are subscripted 1, 2, or 3 to indicate the first, second, or third endothermic peak observed on heating as determined from the calorimeter tracings of the initial heating scans. (See text for structural interpretations.) All samples were initially equilibrated as described in the *Materials and Methods*.

Solvent	Cycle	T_1 (K)	ΔH_1 (kcal/mole)	T_2 (K)	ΔH_2 (kcal/mole)	T_3 (K)	ΔH_3 (kcal/mole)
H_2O	1st Heating	296.5	6.9	311.8	0.8	314.5	7.9
	Cooling			308.6	0.3	314.0	8.3
	2nd Heating			311.8	0.7	314.4	7.8
10 mM $CaCl_2$		360.2	12.5				

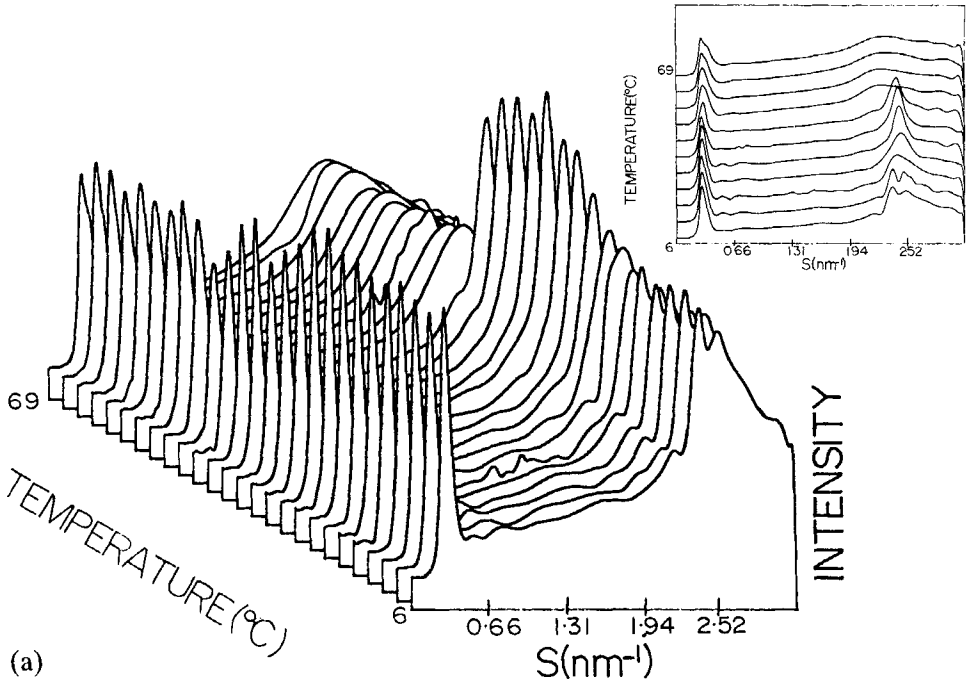

FIGURE 3 X-ray diffraction patterns for DPPG in water undergoing (a) an initial heating scan of 7.9°C/min and (b) a linear re-heating scan of ~7.8°C/min. Every tenth frame of 2s duration of a total data set of 255 frames is shown. *Insets.* Every twenty-fifth frame of the data set is plotted as a function of reciprocal space.

centrations resulted in no observation of a DPPG phase transition in the temperature range studied. The significant rise in the main transition temperature could be explained by the complexation between ions and the DPPG headgroup being strong enough to hinder the thermal destabilization of the ordered bilayer acyl chain packing. One question arises as to whether this is a general situation induced by all salts or a specific influence of Ca^{2+}. A recent study (W. Tamura-Lis, *et al.*, Unpublished observation) has shown that the presence of a fused salt, ethylammonium nitrate, results in a single DPPG transition at approximately 318°K. This would seem to indicate that ion-DPPG complexation eliminates the sub- and pretransitions and raises the temperature of the main phase transition.

CONCLUSIONS

The influence of Ca^{2+} on phospholipid thermodynamic properties can be combined with x-ray diffraction results to describe structural phenomenon related both to Ca^{2+} binding and phase transition parameters. In all cases, the lipids must be initially in the same bilayer packing structure in order to allow for a comparison between different systems. It can be deduced on the basis of thermodynamic data that the binding of Ca^{2+} to DPPG and DPPC clearly changed the structural interactions between lipids within the same bilayer. The increase in the main DPPG phase transition upon the addition of $CaCl_2$ reflects an increase in the acyl chain

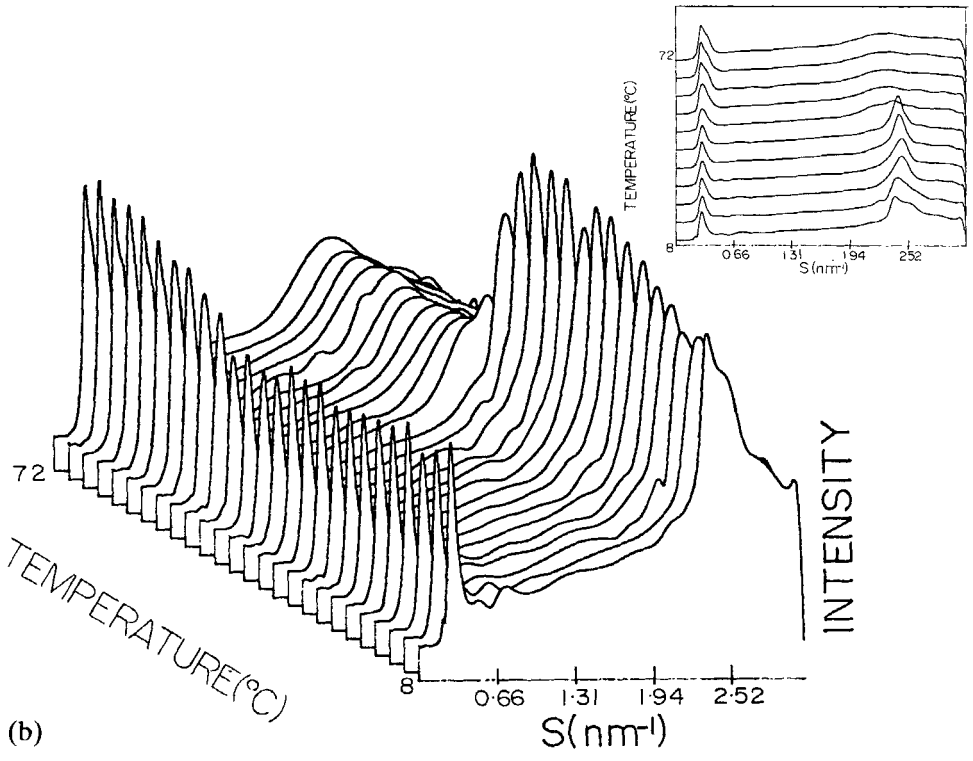

FIGURE 3 (*continued*)

order within the bilayer. The elimination of the DPPC sub transition endotherm with the addition of 50 mM $CaCl_2$ indicates a disordering of the bilayer phase.

Our detailed calorimetric and x-ray diffraction study of the effect of $CaCl_2$ on the DLPE bilayer phases at different temperatures clearly established a biphasic response with increasing $CaCl_2$ concentration. The appearance of two transition endotherms between the DLPE L_c and L_α phases can be related to different populations of lipid in the sample characterized by different temperal or thermal requirements for the transition to proceed. The presence of 10–40 mM $CaCl_2$ results in the appearance of only one DLPE transition endotherm with an enthalpy significantly lower than that of the combined transition enthalpies for DLPE in water, particularly for DLPE in 20 mM $CaCl_2$. X-ray diffraction data obtained as a function

TABLE VI

Structural parameters determined from real time x-ray diffraction patterns for the various phase states formed by DPPG in H_2O

Phase	Mesophase Spacing (nm)	Acyl chain Peak(s) (nm)
L_c	5.61	0.400 0.422
L_β	5.61	0.406 to 0.415
L_α	6.44	0.434

of temperature confirmed the unique phase properties of DLPE bilayers in 20 mM $CaCl_2$ with the observation of a possible supercooled L_α phase. Finally, in the presence of 50 mM $CaCl_2$, DLPE bilayers underwent two distinct thermal transitions, at temperatures different from those observed for DLPE in water. These data were clear indications of the interaction of Ca^{2+} with DLPE, and the subsequent change in the packing within the bilayer as the hydrogen bonding network between DLPE molecules was modified by this interaction.

Acknowledgements

We would like to thank the Glenn H. Brown Liquid Crystal Institute at Kent State University for use of the calorimeter.

References

1. R. V. McDaniel, S. A. Simon, T. J. McIntosh and V. Borovyagin, *Biochemistry*, **21**, 4116–4126 (1982).
2. R. V. McDaniel, T. J. McIntosh and S. A. Simon, *Biochim. Biophys. Acta*, **731**, 97–108 (1983).
3. T. J. O'Leary and I. W. Levin, *Biochim. Biophys. Acta*, **776**, 185–189 (1984).
4. W. Tamura-Lis, L. J. Lis and P. J. Quinn, *J. Phys. Chem.*, **91**, 4625–4627 (1987).
5. S. A. Simon and T. J. McIntosh, *Biochim. Biophys. Acta*, **773**, 169–172 (1984).
6. Y. Inoko, T. Yamaguchi, K. Furuya and T. Mitsui, *Biochim. Biophys. Acta*, **413**, 24–32 (1975).
7. H. Ohshima and T. Mitsui, *J. Colloid. Interface Sci.*, **63**, 525–537 (1978).
8. L. J. Lis, R. P. Rand and V. A. Parsegian, *Biochemistry*, **20**, 1761–1770 (1981).
9. L. J. Lis, W. Tamura-Lis, V. A. Parsegian and R. P. Rand, *Biochemistry*, **20**, 1771–1777 (1981).
10. S. A. Simon, L. J. Lis, J. W. Kauffman and R. C. MacDonald, *Biochim. Biophys. Acta*, **375**, 317–326 (1975).
11. D. Chapman, W. E. Peel, B. Kingston and T. H. Lilley, *Biochim. Biophys. Acta*, **464**, 260–275 (1977).
12. H. Trauble and H. Eibl, *Proc. Nat. Acad. Sci. USA*, **71**, 214–219 (1974).
13. H. Trauble, M. Teubner, P. Woolley and H. Eibl, *Biophys. Chem.*, **4**, 319–342 (1976).
14. A. Watts, K. Harlos, W. Muschke and D. Marsh, *Biochim. Biophys. Acta*, **510**, 63–74 (1978).
15. P. W. M. Van Dijck, B. de Kruijff, A. J. Verkleij, L. L. M. van Deenen and J. DeGier, *Biochim. Biophys. Acta*, **512**, 84–96 (1978).
16. F. Jahnig, K. Harlos, H. Vogel and E. Eibl, *Biochemistry*, **18**, 1459–1468 (1979).
17. A. Watts, K. Harlos and D. Marsh, *Biochim. Biophys. Acta*, **645**, 91–96 (1981).
18. K. Harlos and H. Eibl, *Biochim. Biophys. Acta*, **601**, 113–122 (1980).
19. K. Harlos and H. Eibl, *Biochemistry*, **20**, 2888–2891 (1981).
20. S. Y. K. Wen, D. Hess, J. W. Kauffman, J. M. Collins and L. J. Lis, *Chem. Phys. Lipids*, **32**, 165–173 (1983).
21. J. M. Seddon, K. Harlos and D. Marsh, *J. Biol. Chem.*, **256**, 3850–3854 (1983).
22. J. M. Seddon, G. Cevc and D. Marsh, *Biochemistry*, **22**, 1280–1289 (1983).
23. M. Sacre, W. Hoffman, H. Turner, J. Tocanne and D. Chapman, *Chem. Phys. Lipids*, **25**, 69–83 (1979).
24. P. H. J. Th. Ververgaert, B. de Kruijff, A. J. Verkleij, J. F. Tocanne and L. L. M. van Deenen, *Chem. Phys. Lipids*, **14**, 97–101 (1975).
25. J. M. Boggs and G. Rangarij, *Biochemistry*, **22**, 5425–5435 (1983).
26. D. A. Wilkinson and T. J. McIntosh, *Biochemistry*, **25**, 295–298 (1986).
27. A. E. Blaurock and T. J. McIntosh, *Biochemistry*, **25**, 299–305 (1986).
28. L. J. Lis, W. Tamura-Lis, T. Mastran, D. Patterson, J. M. Collins, P. J. Quinn and S. Qadri, *Mol. Crys. Liq. Cryst.*, **178**, 11–19 (1990).
29. B. G. Tenchov, L. J. Lis and P. J. Quinn, *Biochim. Biophys. Acta*, **897**, 143–151 (1987).
30. C. Nave, J. R. Helliwell, P. R. Moore, A. W. Thompson, J. S. Worgan, R. J. Greenall, A. Miller, S. K. Barley, J. Bradshaw, W. J. Pigram, W. Fuller, D. P. Siddons, M. Deutsch and R. T. Trejear, *J. Appl. Cryst.*, **18**, 396 (1985).
31. J. R. Helliwell, T. J. Greenaugh, P. D. Carr, S. A. Rule, P. R. Moore, A. W. Thompson and J. S. Worgan, *J. Phys.*, E15, 1363 (1982).
32. C. W. Bunn and E. B. Howells, *Nature* (*London*), **174**, 549 (1954).